International Journal of Innovative Research in Science and Engineering
Vol. No.3, Issue 05, May 2017
www.ijirse.com
ISSN (O) 2454-9665
ISSN (P) 2454-0663

"A REVIEW ON CARBON NANOTUBE PROBES FOR MICROSCOPY APPLICATIONS"

Upendra Sharan Gupta[1], Abhishek Chaturvedi[2] , Nishant Patel[3]

Nikhil Kumar Pandey[4]

[1] *Reader Dept. of Mech. Engineering , SVITS, Indore, (India)*

[234]*UG Scholar Dept. of Mech. Engineering ,SVITS, Indore, (India)*

ABSTRACT

Carbon nanotubes have been of great interest because of their simplicity and ease of synthesis. The novel properties of nanostructured carbon nanotubes such as high surface area, good stiffness, and resilience have been explored in many engineering applications. Research on carbon nanotubes have shown the application in the field of energy storage, hydrogen storage, electrochemical supercapacitor, field-emitting devices, transistors, microscopy, nano probes and sensors, composite material, templates, etc. We present a set of ongoing contributions to enhance the performance of AFM (atomic force microscopy) by attaching carbon nanotubes (CNTs) on silicon cantilever tips so that they can work as a probe. Examples of CNT-probed microscopy are reviewed and categorized into two major methods: a gluing method in which CNTs grown somewhere else are bonded on the tips, and a growing method in which CNTs are directly grown from the apex of tips by a CVD (chemical vapour deposition) process. Related topics such as fabrication issues, physics involved during the measurement using as-fabricated probes, improvements in resolution, and limitations of each method are also discussed.

Keywords: Atomic force microscopy , Carbon Nanotubes , Chemical vapour deposition , Probe.

I. INTRODUCTION

Carbon nanotubes (CNTs) emerged in the field of nanotechnology because of their nanosize and unique properties. Carbon nanotubes are hollow cylinders made of graphite carbon atoms with nanoscale (10−9 m) which is much smaller than the human hair width [1]. These CNTs are the members of fullerene structural family with their ends capped with a hemisphere of bucky ball structure [2].

In this era of micro/nano-technology, microscopy techniques become more important in exploring extremely small scale phenomena. AFM (atomic force microscopy) is apparently one of the most widely utilized techniques because it is a very versatile tool for not only measuring the topology of surfaces but also manipulating nanostructures. For example, AFM can be used for lateral arrangements of single atoms or biomolecules to make patterns on a substrate, for tensile tests of carbon nanotubes (CNTs) to study their properties and mechanics, and for electronic applications to data storage devices to develop ultrahigh-density recording system.

Meanwhile, CNT has been attracted great attentions from many researchers because of its high strength, stiffness, variable conductivity, and promising optoelectronic properties for flat display panels. As a result, there

ISSN (O) 2454-9665
ISSN (P) 2454-0663

has been interest to make application with CNTs such as nano-composites[3],[4], nano-scale rotational berings[5], and hydrogen storage media[6].

One of the efforts is made in the area of microscopy studies. Many AFM users realize that the conventional silicon cantilever tip is easily broken when it hits the sample surface by mistakes during the operation. In addition, the fidelity of result is affected by the geometry of the tip so that the topology of high aspect ratio structures often cannot be measured exactly for certain types of pyramidal tips[7]. To solve these problems, a new technique has been proposed such that the cantilever tip has a protruding CNT from its apex, and then the needle-like CNT works as a probe. Since the mechanical property of CNT is very strong, robust and sensitive both chemically and biologically, along with its high aspect ratio geometry that can improve the measurement resolution, the CNT-probed microscopy brought a breakthrough in the development of microscopy technique9.

The ongoing research in this area can be classified into two major groups: a gluing method[10-20] and a growing method[21-23]. In the former method, a readily available CNT is bonded on the point of the silicon tip. For example, Lieber et al.[7] and Dai et al.[8] glued CNTs on silicon tips on which acrylic adhesive is coated. This tip could be used to produce oxide nanostructures, showing high wear-resistance[9]. Similarly, Lieber et al.[10] made CNT-probed tips using UV cure adhesive.

II. THE GLUING METHOD

Bonding readily available CNTs on the apex of the silicon tips is an intuitive and direct method, even though it is somewhat difficult to implement and control due to small size of CNTs and tips. Many research groups have contributed to attaching CNTs to SPM tips, and their approach can be classified into two categories: one is a gluing method in which CNTs are bonded on the tips with coating adhesive, and the other is an attracting method in which CNTs are induced, aligned by the magnetic or electrical field, and finally pulled onto the vertex of tips. The following paragraphs introduce these methods in detail.

Dai et al.[9] firstly showed that carbon nanotubes might be used as ideal probes for scanning probe microscope. The tip employed in their research as shown in Fig. 1 has prolonged life-time and can survive from the inadvertent tip crashes due to its excellent mechanical properties. Another advantage of the tip is that it can image the sharp sloping nanostructures on the surface because of the high aspect-ratio of CNTs. To fabricate the tip, an acrylic adhesive thin film (1-10nm thick) is coated on the bottom 1-2μm section of the conventional silicon tip by slightly measuring the surface of adhesive-coated carbon tape with contact mode. Next, this tip is moved under the view of an optical microscope and brought into contact with the side of a bundle of 5-10 multi-walled carbon nanotubes (MWNTs). Then one MWNT is attached on the tip due to the strong glutinosity of the adhesive. Once after the attachment, the nanotube bundle is withdrawn from the cluster of nanotubes with

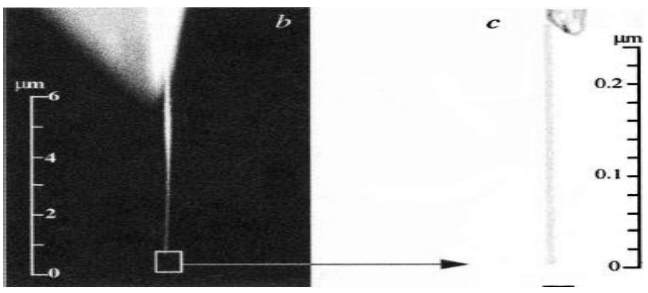

Fig. 1 Single nanotube mounted to the silicon tip(Dai et al.[10])

ISSN (O) 2454-9665
ISSN (P) 2454-0663

tip. Typically, the protruding MWNTs on tips are 5-20nm in diameter and 0.25-1μm in length. In addition, the high wear-resistance can be obtained through the production of oxide nanostructures on them[11]. Similarly, Hafner et al.[12] used UV cure adhesive to fabricate CNT-probed tips.

The tapping mode SFM images of a 400 nm wide, 800 nm deep trench pattern on a silicon wafer are presented in Fig. 2. These images are taken by the silicon tip without and with the CNT respectively. In Fig. 2(a), the apparent triangular shape of the trench can be observed due to the pyramidal shape of the tip. To the contrary, the thin, long nanotubes are now able to reach the bottom of the trench such that they can give clear image of the steep slope structure.

Manual assembly procedure is very time-consuming, which cannot be applied in the large-scale CNT-tips fabrication, in addition, the spatial resolution is limited by the larger diameter of MWNTs, since we can only view the thick nanotubes under the optical microscopy. Lieber et al.[11]found some isolated,

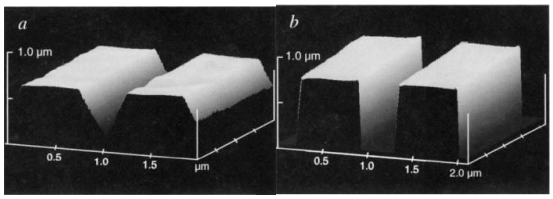

Fig. 2Images of deep trench by (a) silicon tip and (b) CNT-probed tip(Dai et al.[9])

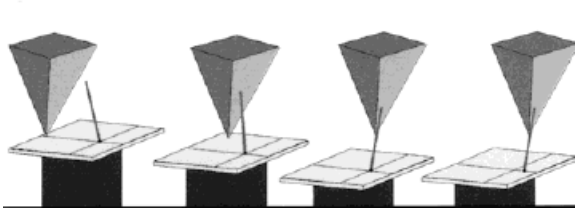

Fig. 3 The process of picking up vertically aligned SWNTs by tips (Hafner et al.[11])

vertically aligned SWNTs stand on the substrate produced by CVD. They attempted to use micro-fabricated silicon tips to pick up individual SWNTs from the substrate. This "pick-up" procedure shown in Fig. 3 is accomplished by imaging the nanotube covered wafers in tapping mode. In order to enhance attachment, the micro-fabricated tips are coated with a layer of UV-cure adhesive at first. After the "pick-up" procedure, the glue is baked in UV light for 30min. The range of SWNT-tips diameters obtained by this method is from 0.9 to 2.8nm. The same literature also introduced how to use electrical etch technique to achieve the great control on the length of SWNTs bonded on tips. A 10-20V, 50-100μs DC pulse are applied between the tip and substrate while imaging a conductive sample. In this procedure, the removal amount from the tip end can be monitored from the change of the sample's z-position. Approximately, 2-5nm length materials will be consistently etched from the tip end per pulse as shown in Fig. 4. In addition, increasing the pulse amplitude can enlarge the length etched per pulse. Nanotubes exhibit field-induced phenomena under magnetic fields[21]. Based on the magnetic properties

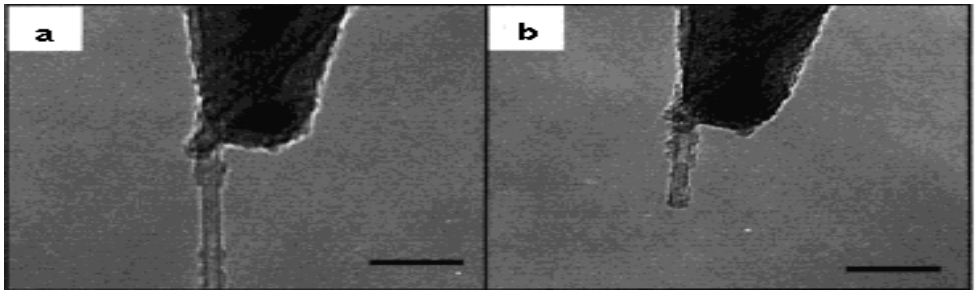

Fig. 4 TEM images of a nanotube tip (a) before and (b) after etching (Hafner et al.[12])

ISSN (O) 2454-9665
ISSN (P) 2454-0663

of CNTs, Hall et al.[15] implemented an apparatus in order to introduce an alternative magnetic field onto a AFM silicon probes and a nanotube suspension (Fig. 5). With this apparatus, the CNTs dispersed in the solution are driven by the applied magnetic field to come into contact with the probe tip, and to protrude preferentially along the magnetic field direction. The AFM tip is fasten by cover slip on the glass cylinder platform, which positions the AFM tip about 400μm from the coil tip. Meanwhile, 5mL of MWNTs suspension in dichloromethane are prepared, and this solution is stirred by ultrasonic bath to achieve maximum homogeneity. The suspension is then dropped into the beaker where the tip is installed. In order to generate induced potential on the AFM tip, a 60nm gold film is sputter-coated on the AFM probe. Then an alternative current of 7A at 60Hz is applied to the coil, resulting in an oscillating magnetic field of amplitude B_0=0.1T. After the coil excitation for 1min, useful CNT-probe tips are obtained with the probability of 50%. In general, these CNTs are found to protrude between 100 and 500 nm from the tip surface and have average 35° deflection angles with respect to the cone axis.

III. THE GROWING METHOD

The "pick and stick" approach of manually attaching nanotubes on silicon pyramid tips is the most widely used method to produce nanotube AFM tips, but this approach is time-consuming manual processes and can fabricate only one tip at a time. Advances have been made by directly growing nanotubes on the AFM tips using chemical vapor deposition (CVD) methods. Compared to the manual assembly, the direct growth can produce higher resolution because the manual assembly is often operated under optical microscopes and only the large nanotube bundles can be seen and attached onto the tip while single-walled CNT with diameter of several nanometers can be grow on AFM tip and the smaller diameter can offer a higher resolution through the direct growth. Another advantage of direct growth is that it can potentially lead to batch production of entire wafers of CNT AFM probes[23],[24].

The idea of growing CNT directly on AFM tips is first reported by Hafner et al[9]. Their approaches are described below:

- Flatten the conventional silicon (Si) tip at its apex by contact AFM imaging;
- Anodize the tip in hydrogen fluoride to create nano-pores of 50–100 nm diameter along the tip axis;
- Electrodeposit iron catalyst into the nano-pores from FeSO4 solution;
- Use Chemical Vapor Deposition (CVD) to grow carbon nanotubes with ethylene and hydrogen at 750 °C for 10 min.

Following the above steps, they can reproducibly form nanotube tips. The direction of the nanotube growth can be controlled by the orientation of the pore structure. The nanotubes are usually too long to be used as tips. They can be shorten by an in situ AFM technique: By applying a voltage pulse, a momentary nano-scale arc is generated between the tip and a conductive surface 10-50nm away, and the tip is shortened by the arc. This method can only roughly adjust the length of nanotube tips, and a more precise method is needed.

Figure 10(a) is a typical field-emission scanning electron microscopy (FE-SEM) image of a nanotube tip after it is shortened. One can see a well-defined tube 480 nm long protruding from the flattened Si tip apex. Through FE-SEM observation, it is found that the nanotubes grown under the same conditions have an

ISSN (O) 2454-9665
ISSN (P) 2454-0663

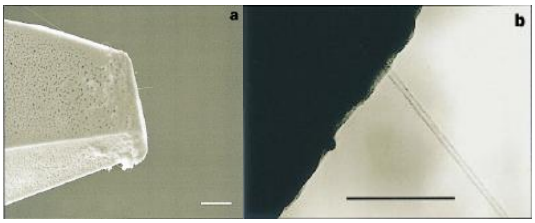

Fig.10 Single-walled CNT grown on apex of average diameter of 10±5 nm. Figure 10(b) is a transmission electron microscopy (TEM) image of the tips showing that they are multi-walled nanotubes (MWNTs) with well-ordered graphite walls.

Later, the same group reported the first growth of single-walled carbon nanotubes (SWNTs) directly from conventional atomic force microscopy (AFM) cantilever assemblies to create very high resolution tips for AFM. A more straightforward method is used to grow nanotubes on AFM tips without apex flattening and pore etching beforehand. The CNTs will grow along the tip surface and reproducibly protrude from the tip apex in the optimal orientation for imaging[19]. Figure 11 shows the scheme of their approaches:

IV. BIOLOGICAL APPLICATIONS

This section presents biological applications of CNT-probed AFM measurement. Many researchers have been studying structural characteristics of biomolecules such as deoxyribonucleic acids (DNAs), chromosomes, and various proteins with AFM that has a conventional silicon tip, but they often face difficulties in obtaining reliable data because of disadvantages inherent in the tip: the radii of tips are still blunt and large so as to measure the topology with exact dimensions of high resolution[19]. Also, the biomolecules are vulnerable to deformation and damage since they are soft materials so that the Si tip results in tip-induced broadening of samples[25]. The durability of the tips is another problem[25]. Although a DNA characterization using a super-sharpened Si tip is reported, it is not very successful in that the tip is unstable and exposed to the risk of being damaged by accidental touch on the surface during the scanning[26].

V. MEASURING FORCES AND DEFORMATION

The inherently high force sensitivity of the AFM cantilever makes it well suited to measuring forces from piconewtons to micronewtons, a range that encompasses many polymer interactions. Force measurements are typically made in two ways: by pulling single molecules to probe molecular-level forces and by indenting polymeric materials to assess their elastic and viscoelastic response to deformation. Single-molecule force spectroscopy involves stretching a molecule between the AFM tip and substrate and measuring the cantilever deflection. With knowledge of the cantilever's spring constant and deflection sensitivity, a plot of force versus distance is obtained. Such force curves provide information about intramolecular forces (e.g., single-chain elasticity, conformational transitions) and intermolecular forces (e.g., polymer-solvent interactions, desorption or adhesion to surfaces) within, or between, single polymer molecules. Figure 5 shows an example of force

International Journal of Innovative Research in Science and Engineering
Vol. No.3, Issue 05, May 2017
www.ijirse.com
ISSN (O) 2454-9665
ISSN (P) 2454-0663

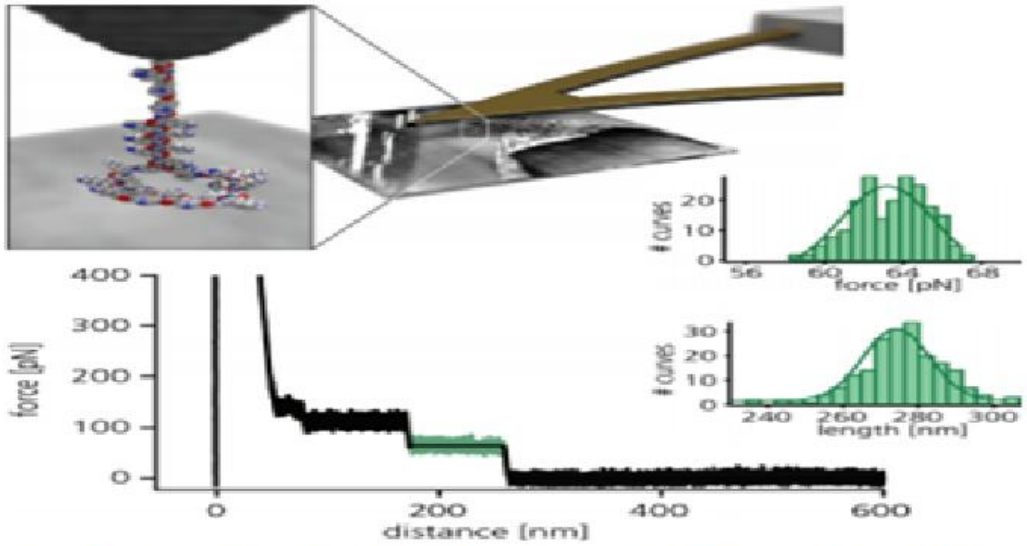

Figure 5: Single molecule forces for poly-L-lysine homopolymer – (top) Graphic of force spectroscopy concepts. A single polymer molecule is covalently attached to the AFM tip by a linker (here, polyethylene glycol, PEG). (bottom) Force-distance curve for poly-L-lysine on a hydrophobic self-assembled monolayer (SAM) in water. The force plateau indicates the desorption of a single polymer from the surface. Histograms obtained from multiple force curves provide the average desorption force (inset, top) and detachment length (inset, bottom). Acquired with the MFP-3D AFM. Adapted from Ref. 29

spectroscopy measurements on molecules of poly-L-lysine as they desorb from a hydrophobic surface.Similarly, AFM indentation measures the cantilever deflection as the tip is pushed into a sample. Conventional cantilevers can apply sufficient forces to deform polymers with modulus in the range from kilopascals to a few gigapascals. Analysis with a model for the tip-sample indentation yields information on the sample's nanoscale elastic and viscoelastic properties .

VI. MEASURING THERMAL PROPERTIES

AFM measurements as a function of temperature provide information on processes such as crystallization, melting, and glass or sub-glass transitions. Sample heating stages enable controlled, variable temperature over the range of interest for polymer transitions. Figure 8 shows the temperature dependence of modulus in polyethylene terephthalate, a thermoplastic polyester. Figure 9 shows the morphology changes of a shape memory microparticle as it is heated.Besides monitoring morphology and material properties as a function of temperature, techniques also exist to directly probe thermal properties at the nanoscale. Scanning thermal microscopy (SThM) is a technique that operates in contact mode with a special cantilever that monitors the temperature changes from a local heat source. By measuring the local surface temperature of the sample, it generates image contrast that depends on the local thermal conductivity. Figure 10 shows a polymer blend imaged using SThM.Local thermal analysis (LTA) is another thermal technique. Rather than sensing the sample temperature like SThM, it instead uses a locally heated probe to heat a nanoscale volume of the sample.As the sample heats or cools, it expands or contracts according to the local coefficient of thermal expansion. This effect is measured by deflection of the cantilever, resulting in deflection versus temperature curves. These curves are a sensitive tool to measure the onset of thermal transitions in the material and can be used to distinguish different

International Journal of Innovative Research in Science and Engineering
Vol. No.3, Issue 05, May 2017
www.ijirse.com
ISSN (O) 2454-9665
ISSN (P) 2454-0663

materials based on their melting or glass transition temperatures. Figure 11 shows this technique applied to a ternary polymer blend.

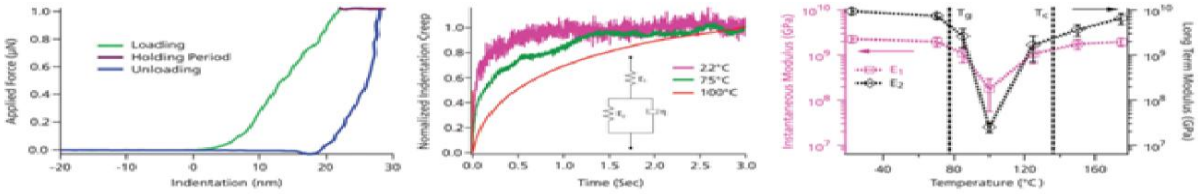

Figure 8: Temperature dependence of PET viscoelastic properties – *(left) Force curve for polyethylene terephthalate (PET). A 3 second hold segment of constant force was applied between the force loading and unloading cycles. (center) Creep curves of indentation versus time during the force curve hold interval. The curves have been normalized to vary between zero and one, highlighting the increase in relaxation time with temperature. (right) Temperature dependence of instantaneous modulus E_1 (pink squares) and long term modulus E_2 (black diamonds) obtained by fitting the creep curve to a three-element Maxwell-Voigt model (inset, center). Both E_1 and E_2 exhibit a dramatic drop in the temperature range between the glass-to-rubber transition temperature $T_g \approx 77°C$ and the PET crystallization temperature $T_c \approx 135°C$ due to the film's semicrystalline nature in this range. Acquired with the MFP-3D AFM and PolyHeater sample stage. Adapted from Ref. 30*

Figure 9: Annealing of shape memory polymer – *Tapping mode topography images of a polystyrene (PS) microparticle during annealing. Scan size 12 μm, Z (height) scale 1.4 μm. The PS particle was flattened with a high-temperature, high-pressure nanoimprint lithography (NIL) process and then thinly coated with gold. Imaging began with the particle heated to 80°C. The heater temperature was rapidly increased to 102°C and then increased stepwise, so that it was 106°C after 78 min. and 110°C at 170 min. During annealing the particle diameter decreases and the height increases, recovering the original, pre-NIL spherical shape. A surface wrinkling morphology develops that gives information on recovery dynamics and strain energy release. Applications for micro- and nanoscale polymer particles include drug delivery and electronic packaging; incorporating shape memory effects could lead to many more. Imaged with the MFP-3D AFM. Adapted from Ref. 31*

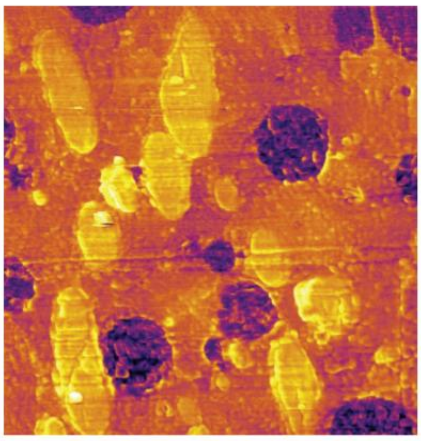

Figure 10: SThM on PP-PS-PE ternary blend – *The sample contained 60% polypropylene (PP), 20% polystyrene (PS), and 20% polyethylene (PE) by weight. In this SThM image, the three components are clearly distinguished, with darker colors corresponding to higher thermal conductivity. As expected from literature values for their thermal conductivity, the oblong regions of PS are brightest (yellow, 0.03 W/m·K), the circular regions of PE are darkest (purple, 0.4 W/m·K), and the surrounding PP matrix is intermediate (orange, 0.12 W/m·K). Imaged with the MFP-3D AFM; scan size 15 μm. Sample courtesy of Dalia Yablon and Andy Tsou, Corporate Strategic Research, ExxonMobil Research and Engineering.*

ISSN (O) 2454-9665
ISSN (P) 2454-0663

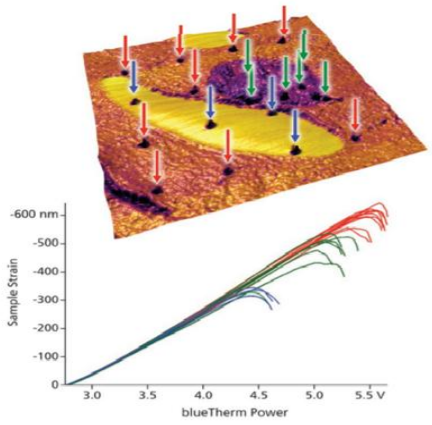

Figure 11: LTA of PP-PE-PS ternary blend *– (top) AM-FM Viscoelastic Mapping Mode image of the same sample used in Figure 10. The brighter colors indicate higher modulus. Scan size 6 µm. The black dots indicate points where LTA measurements were made. (bottom) The LTA measurements are color coded with the points in the image and clearly distinguish the different transition temperatures for PS (blue), PE (green) and PP (red). Sample courtesy of Dalia Yablon and Andy Tsou, Corporate Strategic Research, ExxonMobil Research and Engineering.*

VII. CONCLUSION

Investigations on the characteristics of CNT-attached AFM cantilever are reviewed with regard to fabrication issues, structural mechanics, improvements in resolution, and biological applications. Two methods – growing and gluing – of producing a CNT tip on a silicon pyramid are studied, and dimension measurements of biomolecules are illustrated.

REFERENCES

[1]Michael F, De Volder L, Tawfick SH, Baughman RH, John Hart A. Carbon nanotubes: present and future commercial applications**.** *Science. 2013;339:535–9.*

[2]Chen H, Liuyang Z, Matthew B, Hong N, Jinbao C, Xianqiao W. Molecular dynamics study of a CNT–buckyball-enabled energy absorption system.*Phys Chem Chem Phys. 2015;17:17311–21***.**

[3] V. Lordi, N. Yao, *J. Mater.*Res. **15**(12), 2770-2779 (2000).

[4] E.T. Thostenson, Z. Ren, T.W. Chou, *Composit. Sci.* Tech. **61**, 1899-1912 (2001).

[5] S. Zhang, W.K. Liu, R.S. Ruoff, *Nano Lett.***4**(2), 293-297 (2004).

[6] G. Stan, M.W. Cole, *J. Low Temp. Phys.***110**, 539-544 (1998).

[7] S.S. Wong, A.T. Woolley, T.W. Odom, J.L. Huang, P. Kim, D.V. Vezenov, C.M. Lieber, *Appl. Phys. Lett.***73**(23), 3465-3467 (1998).

[9] H. Dai, J.H. Hafner, A.G. Rinzler, D.T. Colbert, R.E. Smalley, *Nature***384**(14), 147-150 (1996).

[10] H. Dai, N. franklin, J. Han, *Appl. Phys. Lett.***73**(11), 1508-1510 (1998).

[11] J.H. Hafner, C.L. Cheung, T.H. Oosterkamp, C.M. Lieber, *J. Phys. Chem. B.***105**(4), 743-746 (2001). [12] H. Nishijima, S. Kamo, S. Akita, Y. Nakayama, K.I. Hohmura, S.H.Yoshimura, K. Takeyasu, *Appl. Phys. Lett.***74**(26), 4061-4063 (1999)

[13] S. Akita, H. Nishijima, Y. Nakayama, F. Tokumasu, K. Takeyasu, *J. Phys. D: Appl. Phys.***32**, 1044-1048 (1999).

ISSN (O) 2454-9665
ISSN (P) 2454-0663

[14] J. Tang, G. Yang, Q. Zhang, A. Parhat, B. Maynor, J. Liu, L.-C. Qin, O. Zhou, *Nano Lett.***5**(1), 11-14 (2005).

[15] A. Hall, W.G. Matthews, R. Superfine, M.R. Falvo, S. Washburn, *Appl. Phys. Lett.***82**(15), 2506-2508 (2003).

[16] C.V. Nguyen, R.M.D. Stevens, J. Barber, J. Han, M. Meyyappan, M.I. Sanchez, C. Larson, W.D. Hinsberg, *Appl. Phys. Lett.***81**(5), 901-903 (2002).

[17] R. Stevens, C. Nguyen, A. Cassell, L. Delzeit, M. Meyyappan, J. Han, *Appl. Phys. Lett.***77**(21), 3453-3455 (2000).

[18] J.H. Hafner, C.-L. Cheung, C.M. Lieber, *Nature***398**(29), 761-762 (1999).

[19] J.H. Hafner, C.L. Cheung, C.M. Lieber, *J. Am. Chem. Soc.***121**, 9750-9751 (1999).

[20] E.B. Cooper, S.R. Manalis, H. Fang, H. Dai, K. Matsumoto, S.C. Minne, T. Hunt, C.F. Quate, *Appl. Phys. Lett.***75**(22), 3566-3569 (1999).

[21] J.P. Lu, *Phys. Rev. Lett.***74**(7), 1123-1126 (1995).

[22] A. Brioude, P. Vincent, C. Journet, J.C. Plenet, S.T. Purcell,*Appl. Surf. Sci*. **221**, 4-9(2004).

[23] E. Yenilmez,Q. Wang, R.J. Chen, D. Wang, H. Dai, *Appl. Phys.Lett.***80**, 2225-2227 (2002).

[24] Q. Ye, A.M. Cassell, H. Liu, K.J. Chao, J. Han, M. Meyyappan, *Nano Lett.***4**(7), 1301-1308 (2004).

[25] Y.C. Chang, C.S. Chang, D.C. Wang, M.-H. Lee, T.-F. Wang, M.-Y. Wu, T.-Y. Fu, T.T. Tsong, *Jpn. J. Appl. Phys.***43**, 4517-4520 (2004).

[26] T. Uchihashi, N. Choi, M. Tanigawa, M. Ashino, Y. Sugawara, H. Nishijima, S. Akita, Y. Nakayama, H. Tokumoto, K. Yokoyama, S. Morita, M. Ishikawa, *Jpn. J. Appl. Phys.***39**, L887-889 (2000).

[27] S.S. Wong, J.D. Harper, P.T. Lansbury, Jr., C.M. Lieber, *J. Am. Chem. Soc.***120**, 603-604 (1998). [28] L. Chen, C.L. Cheung, P.D.Ashby, C.M. Lieber, *Nano Lett.***4**(9), 1725-17.

[29] S. Kienle, T. Pirzer, S. Krysiak, M Geisler, and T. Hugel,Faraday Discuss. 160, 329 (2013).

[30]. C.A. Grant, A. Alfouzan, T. Gough, P.C. Twigg, andP.D. Coates, Micron 44, 174 (2013).

[31]. L.M. Cox, J.P. Killgore, Z. Li, Z. Zhang, D.C. Hurley, J. Xiao,and Y. Ding, Adv. Mater. 26, 899 (2013).